Int. J. Electrochem. Sci., 8 **(2013)** 5594 - 5604

International Journal of
ELECTROCHEMICAL
SCIENCE
www.electrochemsci.org

Structural and Optical Characterization of Cu and Ni Doped ZnS Nanoparticles

Khalid T. Al- Rasoul[2], *Nada K.Abbas*[1,*], *Zainb J. Shanan*[1]

[1] College of science for Women, University of Baghdad, Jadriya, Baghdad, Iraq
[2] College of science, University of Baghdad, Jadriya, Baghdad, Iraq
[*]E-mail: nadabbs@yahoo.com

Received: 6 February 2013 / *Accepted:* 14 March 2013 / *Published:* 1 April 2013

Doped zinc sulfide nanoparticles with nickel and copper with different ratios were synthesized from mixture of zinc acetate nickel chloride and copper chloride with sodium sulfide in aqueous solution. The X-ray diffraction patterns showed the typical inter planer spacer corresponding to the cubic phase. Crystallographic studies show the zinc blend crystals varies average crystallite size approximated 4.27 and 4.56 nm for ZnS: Cu and ZnS: Ni respectively, which is almost similar to the average particle size calculated from effective mass approximation .UV-vis spectrophotometer measurements blue shift for both doping elements.

Keywords: Nano particles of (ZnS:Cu) &(ZnS:Ni), The characterization of (ZnS:Cu and Zns:Ni): absorption, photoluminescence spectra, x-ray diffraction and atomic force microscopy

1. INTRODUCTION

Research on semiconductor nanoparticles stimulated great interest in recent years because of their unique optical and electrical properties. Among the semiconductor nanoparticles, zinc sulfide as an important II–VI semiconductor has been researched extensively because of its broad spectrum of potential applications such as in catalysts, cathode-ray tubes (CRT), field emission display (FED) phosphors for a long time. It can also be used for electroluminescent devices and photodiodes [1, 2]. In recent years, much effort has been devoted to the research of doped metal chalcogenide nanostructured materials. This kind of nanomaterials exhibits unusual physical and chemical properties in comparison with their bulk materials, such as size-dependent variation of the band gap energy. Furthermore, impurity ions doped into these nanostructures can influence the electronic structure and transition probabilities [3]. In particular, when doped with magnetic ions (e.g. Mn2+), these materials can

produce unique magnetic and magneto-optical properties and provide unparalleled opportunities for the new field of spintronics [4].

As an important II–VI semiconductor material, ZnS is chemically more stable and technologically better than other chalcogenides (such as ZnSe), so it is considered to be a promising host material. Transitional elements ions (e.g. Mn^{2+}, Ni^{+2} and Cu^{2+} [1, 3-11]) and rare earth ions (e.g. Eu^{2+} [12, 13]) have been incorporated into ZnS nanostructures by thermal evaporation, sol–gel processing, co precipitation, micro emulsion, etc. These doped ZnS semi-conductor materials have a wide range of applications in electro-luminescence devices, phosphors, light emitting displays, and optical sensors.

The aim of this paper is to report the result of investigations on the synthesis x-ray diffraction, uv-vis absorption, atomic force microscopy (AFM) and photoluminescence (PL) studies of undoped and Cu, Ni doped ZnS nanoparticles.

2. EXPERIMENTAL

ZnS: Cu and ZnS: Ni nanocrystals have been synthesized using wet chemical co-precipitation method at room temperature. Analytical reagent grade chemicals zinc acetate ($C_4H_6O_4Zn.2H_2O$) copper chloride ($CuCl_2$), nickel chloride ($NiCl_2$) and sodium sulfide ($Na_2S.H_2O$) were used without further purification. Solution of 0.1 M zinc acetate, 0.1M sodium sulfide and 0.01M each of Cu and Ni chloride were prepared in separated flask.

I n a typical synthesis 5ml Zn $(Ac)_2$ (0.1M) was mixed with (1,3,and 5 ml) of 0.01M Cu and Ni at room temperature . 10 ml Na_2S slowly added with stiring to the above mixture .The synthesized powders separated from the solution with a centrifugation at 3000 rpm .The samples were washed three times with ethanol.

The crystalline structure, phase purity and size of the nanoparticles were determined by X-ray powder diffraction technique. The X-ray powder diffractometer (Shimat Zo) with nickel filtered monochromated CuKα radiation (λ=1.5406˚A).The samples were scanned over the required range for 2θ values (20-60˚) .The optical absorption measurements obtained from the colloidal solution were performed in UV-Vis spectrophotometer SP-3000 plus, OPTIMA INC. Japan, the nanopowders were first dispersed in methanol and then taken on a quartz cuvette of path length 10mm. The PL spectrum of the ZnS has been measured at room temperature using Hitachi F-2500 FL Spectro-photometer. For measuring the PL intensity, the nanopowders were first dispersed in methanol and then taken on a four side polished quartz cuvette of path length 10 mm.In order to investigate the surface morphology and surface roughness, the atomic force microscopy (AFM) observations were performed using an an SPM model AA 3000, Angstrom Advanced Ins.,USA . The AFM images were analyzed with the Pro Scan software (Park Scientific Instruments), calculating the root mean square surface roughness value.

3. RESULTS AND DISCUSSION

3.1 XRD studies

The Cu and Ni doped ZnS nanoparticles were characterized by X-ray powder diffraction. The X-ray diffraction patterns of nanoparticles are shown in Fig.(1).From fig. 1 the X-ray peaks have been found to correspond to (111), (220), and (311) planes of the pure ZnS cubic phase (JCPDS 05-0566). The structure of ZnS remains virtually unchanged by the incorporation of the dopants but the peaks got broadened. In all patterns no peaks corresponding to impurities were detected. Broadening of undoped and doped samples indicates the formation of ZnS nanocrystals.

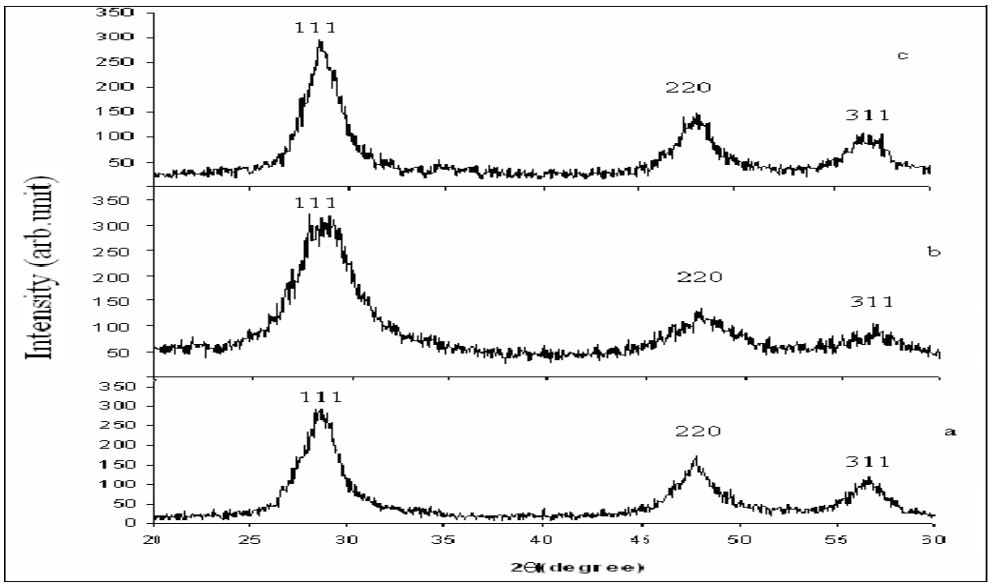

Figure 1. XRD of (a) ZnS, (b) ZnS:Cu and (c) ZnS:Ni nanoparticles.

Table 1. Crystallite size variation with dopant materials

Sample	Crystallite size(nm)
Undoped ZnS	4.59
ZnS:Cu	4.27
ZnS:Ni	4.56

To calculate the nanoparticle diameter from the width of the line in the XRD spectrum, the Scherrer formula [10, 11].

$$D= \frac{0.9\lambda}{\beta \cos\theta} \text{.....(1)}$$

Where D is the mean particle size, λ is the wavelength of incident X-ray (1.5406 ˚A), θ is the degree of the diffraction peak , and β is the full width at half maximum (FWHM)of the XRD peak appearing at the diffraction angle θ. The mean calculated crystallite size of the undoped ZnS and doped with Cu and Ni nanoparticles shows that the synthesized nanoparticles are in the quantum confinement regime as given in table (1) .Those results are in agreement with literature [1, 3, 8, and 10].

3.2 Optical properties

Figs. 2 show UV–Vis spectra of the Cu-doped ZnS and undoped ZnS nanoparticles. The absorption peak at 290 nm in the curve of un-doped sample is attributed to the absorption of ZnS nanoparticles. With the Cu doping concentration increased the absorption edge shifted to blue edge from 290, 288, and 285 to 280 nm.

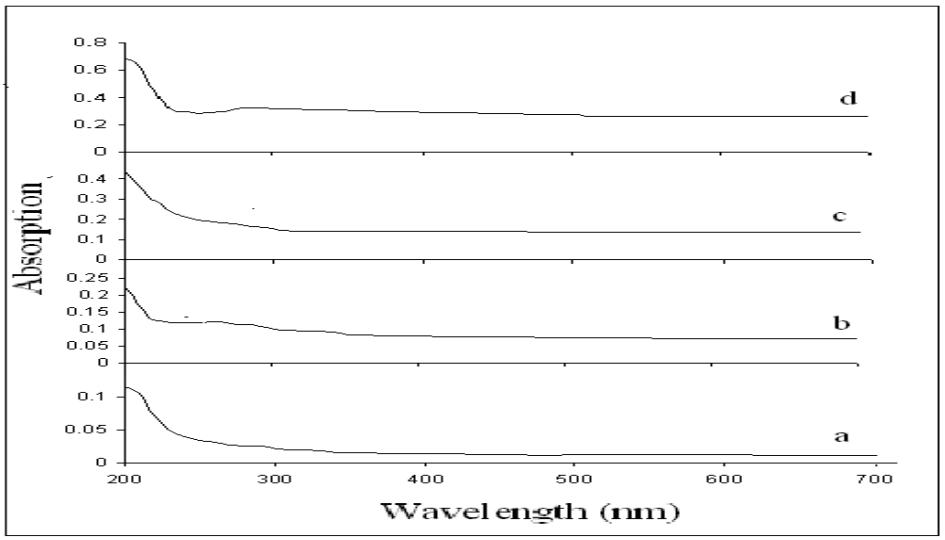

Figure 2. Absorption spectra for ZnS (a) and ZnS:Cu nanoparticles with Cu doping concentrations 1 ml (b), 3 ml (c),(d) 5 ml respectively.

The UV-Vis absorption spectra Fig. 3 of the synthesized undoped and Ni-doped ZnS nanoparticles have been recorded, to measure their band-gap. The spectra show absorption edge of the nanoparticles in the range - 290 to 270 nm, showing these nanoparticles being blue-shifted as compared to bulk ZnS for which the peak is at 340 nm. The blue shift in the absorption edge is due to the quantum confinement of the excitons present in the sample, resulting in a more discrete energy spectrum of the individual nanoparticles. The effect of the quantum confinement on impurity depends upon the size of the host crystal. As the size of the host crystal decreases, the degree of confinement and its effect increases [8]. On doping Ni in the ZnS nanoparticles, the blue shift further increases, which might be due to the fact Ni forming new energy levels in the ZnS energy band. Using equation 2 and 3, the band-gap and average particle size of ZnS and ZnS:Ni nanoparticles have been calculated.

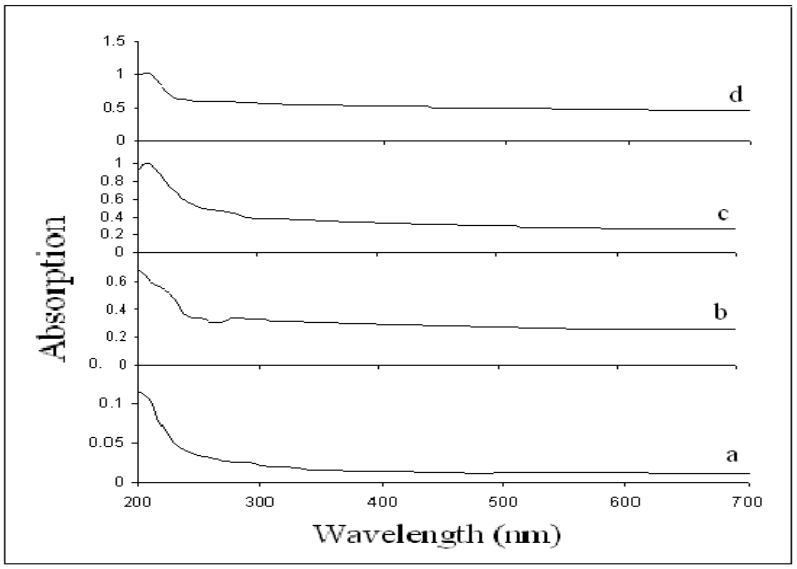

Figure 3. Absorption spectra for ZnS (a) and ZnS:Ni nanoparticles with Ni doping concentrations 1 ml (b), 3 ml (c),(d) 5 ml respectively

The band gap energy in a nanomaterial could be obtained from the absorption maxima. According to quantum confinement theory, electrons in the conduction band and holes in the valence band are spatially confined by the potential barrier of the surface. Due to confinement of both electrons and holes, the lowest energy optical transition from the valence to conduction band will increase in energy, effectively increasing the band gap (Eg) [14]. The shoulder or peak of the spectra corresponds to the fundamental absorption edges in the samples, and could be used to estimate the band gap of the nanomaterial [15]. Due to quantum size effects the band gap energy increases with decreasing particle size. [11, 16].

From the absorption peak the optical energy band gap of ZnS nanostructure has been calculated using the formula:

$E_{gn} = h\nu_{gn} = hc/\lambda_{gn}$ ……. (2)

where h=plank's constant and *Egn* = energy band gap of the semi conducting nanoparticles in the optical spectra .To calculated band-gap value of the nanoparticles for undoped ZnS was 4.27 eV, which is blue shifted from that of bulk ZnS (340 nm, Eg = 3.65 eV). Increasing of band gap energies of ZnS nanostructures could be an indication of the quantum confinement effect due to decreasing size of structures. The average particle size present in the nanocolloid can be determined by using the mathematical model of effective mass approximation [14].The following equation derived, describes the particle size (*r* , radius) as a function of peak absorbance wavelength (λp) for ZnS nanocrystals [16,17].

$$r(nm) = [\{-0.2963 + (-40.1970 + 13620/\lambda_p)^{1/2}\}/\{-7.34 + 2481.6/\lambda_p\}]\text{^}2 \ldots\ldots (3)$$

The energy gap and average particle size for undoped ZnS and Cu doped ZnS are listed in table 2.We observed from table 2 the particle size decrease with doped ZnS and increasing concentration of Cu. .Our results agreement with [15].

Table 2. Energy gap and Average particles of ZnS: Cu, ZnS: Ni and ZnS.

Cu concentration (ml)	ZnS:Cu		ZnS:Ni	
	Energy gap (eV)	Average particle size (nm)	Energy gap (eV)	Average particle size (nm)
0	4.27	3.8	4.27	3.8
1	4.3	3.7	4.36	3.56
3	4.4	3.6	4.42	3.4
5	4.42	3.4	4.54	3.22

3.4. Photoluminescence study

The room temperature photoluminescence (PL) spectra of ZnS, ZnS: Cu and ZnS: Ni nanoparticles at an excitation wavelength of 250 nm are illustrated in Figs.4 and 5 respectively. The spectra are broad and asymmetric, so it should consist of more than one component. The PL spectrum of the undoped ZnS nanoparticles and Cu and Ni doped ZnS nanoparticles were deconvoluted into two peaks, which are listed in Table 3. Our result agreement with [18].

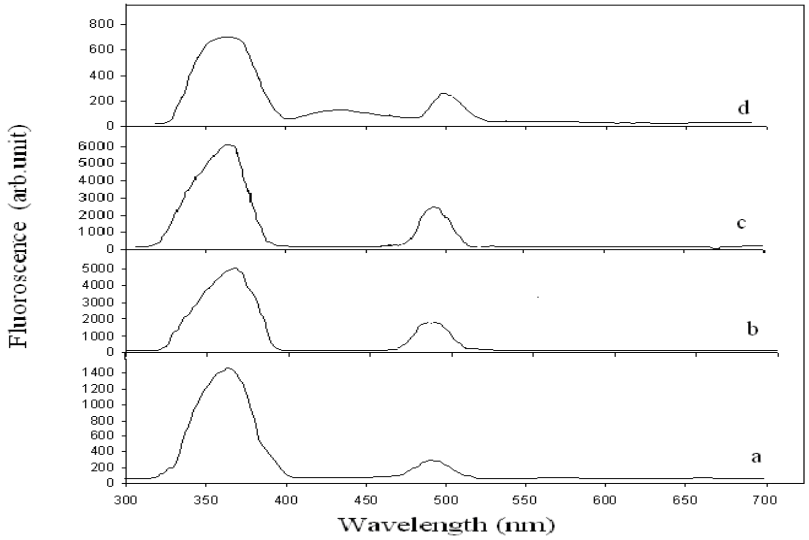

Figure 4. Room temperature photoluminescence spectra of the ZnS nanoparticles with Cu^{2+} concentrations (a) 0, (b) 1 ml, (c) 3 ml, and (d) 5 ml.

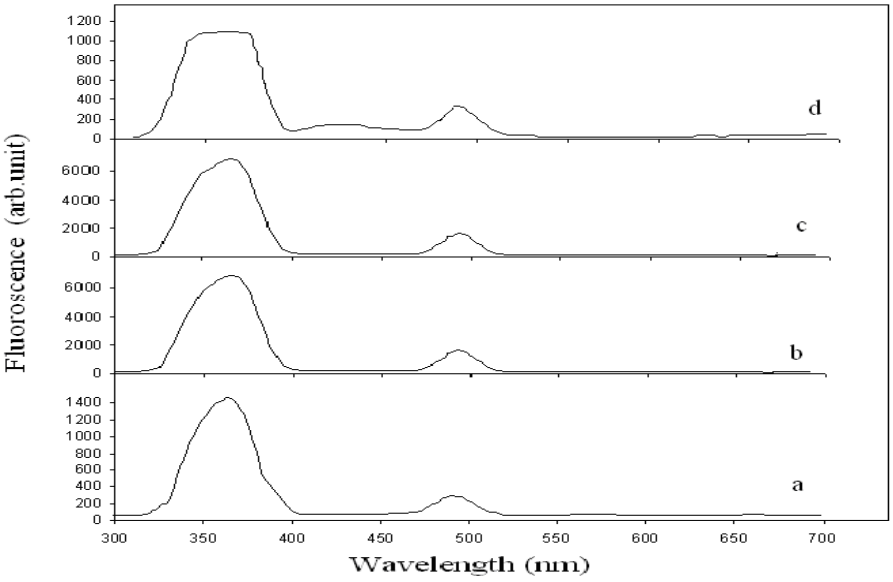

Figure 5. Room temperature photoluminescence spectra of the ZnS nanoparticles with Ni^{2+} concentrations (a) 0, (b) 1 ml, (c) 3 ml, and (d) 5 ml.

In fig. 4 the peak at 367 nm (3·37 eV) can indicate exciton recombination, the emission at 491 nm may be caused by the transition from the con The emission at 491 nm may be caused by the transition from the conduction band to the zinc vacancies V_{Zn} level (this localized vacancy level is above the valence band at 1.1 eV [19]. As shown in Table 3, the peak position of this blue emission does not change with the increase of the Cu^{2+} concentration, which indicates that the energy level of zinc vacancy relative to the conduction band nearly keeps constant. Generally speaking, the emission spectra of Cu-doped ZnS were reported quite different by different authors because of different quantum particle size, surface or impurity defect levels in the band gap, caused by different synthesis techniques.

Table 3. Photoluminescence peak positions in the ZnS and ZnS:Cu nanoparticles

Cu concentration (ml)	PL peak positions of ZnS:Cu		PL peak positions of ZnS:Ni	
	Peak I (nm)	Peak II (nm)	Peak I (nm)	Peak II (nm)
0	367	491	367	491
1	369	495	365	493
3	367	493	363	491
5	368	499	367	489

Usually, the luminescence mechanism of Cu^{2+} doped ZnS is described as follows: Cu^{2+} ions formed deep trap energy levels between valence band (VB) and conduction band (CB) of ZnS. By

absorbance of external energy, electrons are excited from VB to CB and relax to shallow defect levels formed by impurity ions. The activated electrons will recombine with holes left in the CB or the holes transferred to Cu^{2+} trap energy levels by radiative transition, which give out photons. So it is possible to observe the emission from ZnS and Cu^{2+} centers at the same time. The energy levels of the dopant, Cu^{2+} ions, varied with the doping concentration and slightly different emission wavelength can be observed. From the luminescent mechanism, it is positive that Cu^{2+} substitute Zn^{2+} in the lattice [20].

From fig.5 observed that PL emission band from undoped ZnS nanoparticles are broaden with two peaks and Ni^{2+} doped ZnS. In the PL process, an electron from the valence band is excited across the band gap and photo excited electron subsequently decays by a normal recombination process to some defect states. In Ni doped crystals an electron may be captured by the Ni^{2+} ions in the $^4T_1$ level, from which it makes a radiative transition to the ground state $^6A_1$level [10]. The peaks at 489 to 92.5 nm may be due to the zinc vacancy related defects [19].

3.5 Surface morphology

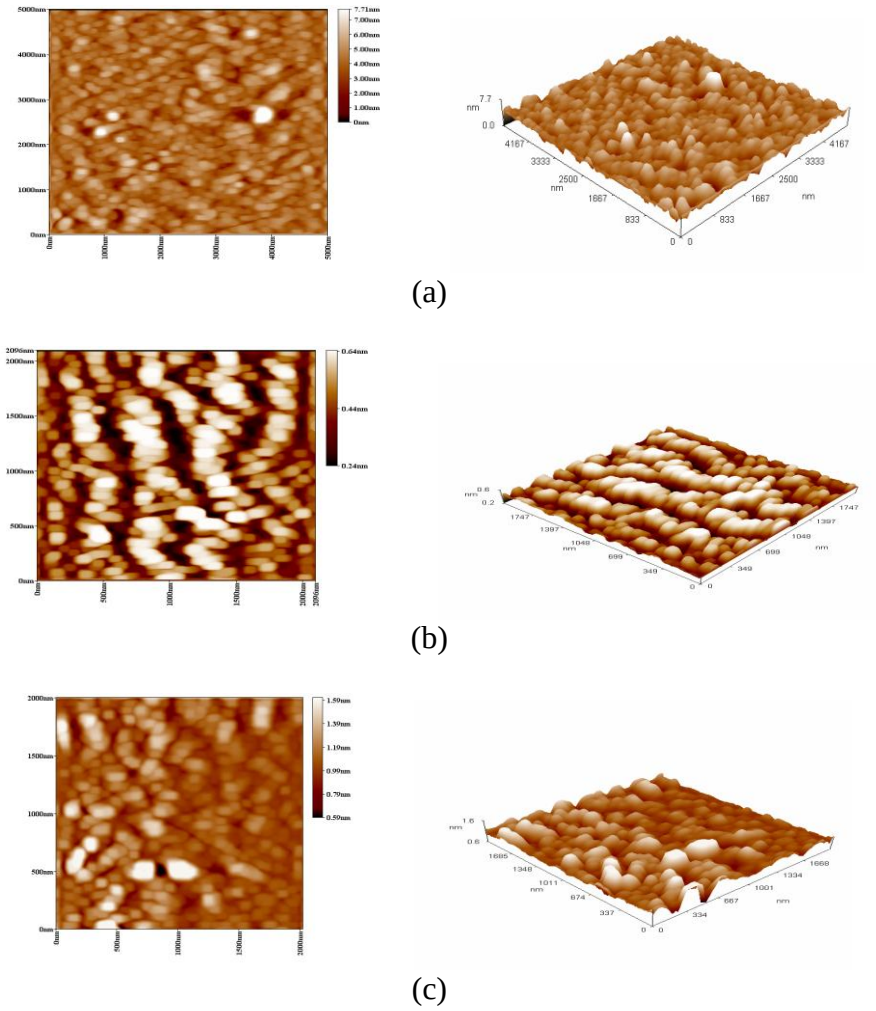

Figure 6. AFM images of ZnS:Cu powder placing on glass. Two-dimensional and three – dimensional. (a) 1 ml **(b)** 3 ml (c) 5 ml

Atomic force microscopic (AFM) allows us to get microscopic information on the surface structure and to plot topographies representing the surface relief.

This technique offers digital images, which allow quantitative measurements of surface features, such as root mean square roughness, *Rq*, or average roughness *Ra*, and the analysis of images from different perspectives, including three-dimensional simulation [21].

Fig. (6, 7) illustrates two and three dimensional AFM images of the ZnS: Cu and ZnS: Ni.AFM measurement obtained by placing a drop of colloidal solution on glass.

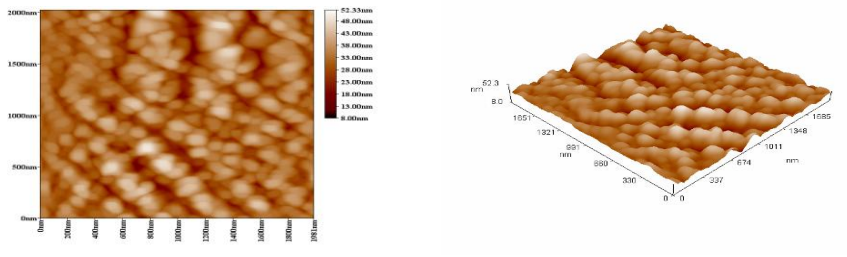

(a)

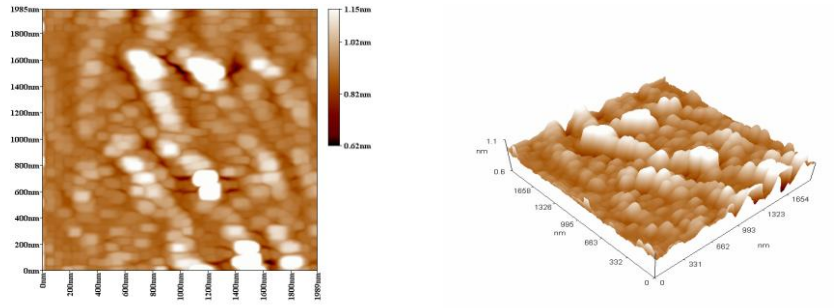

(b)

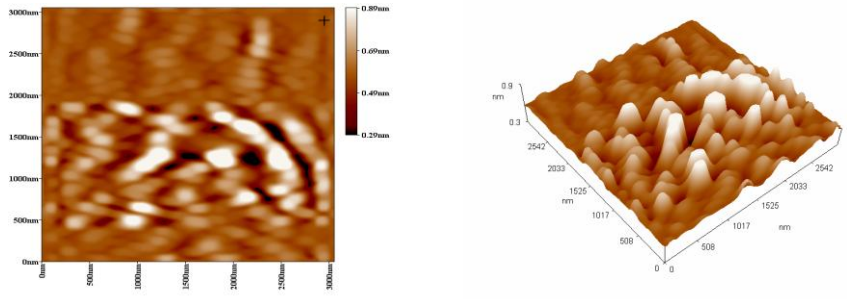

(c)

Figure 7. AFM images of ZnS:Ni powder placing on glass. Two-dimensional and three – dimensional. (a) 1 ml **(b)** 3 ml (c) 5 ml

Average grain size in diameter of ZnS: Cu (1, 3 and 5 ml) and ZnS:Ni (1, 3, 5 ml) were listed in Table 4. It is important to note that these obtained values are averaged and there is a statistical variation associated with them, which depends on the location of the measurements that are performed on the samples [22].

Table 4. Average grain size of ZnS: Cu and ZnS: Ni nanoparticles.

Concentration (ml)	ZnS:Cu Average grain size	ZnS:Ni Average grain size
1	89.37	98.88
3	85.21	83.61
5	65.63	73.18

We observed from table.4, that average grain size decrease with increasing concentration of doping for all samples. That is agreement with optical measurements.

4. CONCLUSION

In conclusion, we have successfully synthesized the ZnS:Cu and ZnS:Ni nanoparticles by a simple aqueous chemical method using pure aqueous route resulting in primary particle sizes average about 4.26 and 4.56 nm respectively . These particles sizes were calculated from the Debye- Scherrer formula and effective mass approximation. AFM image is used to study the morphology of the synthesized nanoparticles. UV spectra revealed that the absorption band was blue shifted from the bulk. Photoluminescence investigation evidenced the high crystalline nature of the ZnS nanoparticles.We observed from above results that result's Cu doped ZnS close near from result's Ni doped ZnS.

References

1. H.Wang , X. Lu, Y. Zhao and C. Wang ,*Materials Letters* , 60 (2006) 2480.
2. N. Habubi, M. Hashim and A. Al-Yasiri, *Baghdad Science Journal*, 7 (2010) 1421.
3. W. Peng , G. Cong, S. Qu and Z. Wang, *Optical Materials* ,29 (2006) 313.
4. D. Awschalom and J. Kikkawa, *Phys. Today* ,52 (1999) 33.
5. J. Tolia, M. Chakraborty, and Z. Murthy, *International Journal of Chemical Engineering and Applications*, 3 (2012) 136.
6. B. Rema Devi, R. Veendran and A. Vaidyan , *journal of physics* , 68(2007) 679.
7. R. Sarkar, C. Tiwary, P. Kumbhakar , S. Basu and A.K. Mitra , Physica E 40 (2008) 3115.
8. S. Kumara, N. Verma and M. Singla ,*Chalcogenide Letters* , 8 (2011) 561.
9. A. Firdous, T. Rasool, G. Dar and M. Ahmad, *Journal of Optoelectronics and Biomedical Materials*, 2 (2010) 175.
10. C. Pthak, P. Pathk, P. Kumar, M. Mandal, *Journal of Ovonic Research* , 8 (2012) 15.
11. A. Bol, J.Ferwerda, J. Bergwerff and A. Meijerink , *Journal of Luminescence*, 99 (2002) 325.
12. W. Chen, J. Malm, V. Zwiller, Y. Huang, S. Liu, R. Wallenberg, J. Bovin and L. Samuelson, *Phys. Rev.* 61 (2000) 11021.

13. S. Xu, S. Chua, B. Liu, L. Gan, C. Chew and G. Xu, *Appl. Phys. Lett.* 73 (1998) 478.
14. D. Onwudiwe and P. Ajibade *Int. J. Mol. Sci.* , 12 (2011) 5538.
15. T. Hoa, L. Vu, T. Canh and N. Long, *J. Phys.*, 187 (2009) 012081.
16. A. Tiwari, S . Khan and R. Kher, *Advances in Applied Science Research*, 2 (2011) 105.
17. A. Tiwari, S. Khan and R. Kher, Bull. Mater. Sci., 34 (2011) 1077.
18. S.J.Xu, S.J.Chua, B.Lui, *Appl. Phys.Lett*, 73 (1998) 478-480.
19. N. Abbas, K. Al- Rasoul and Z. Shanan. *J.Int.Electrochem.Sci*, 8 (2013) 3049.
20. M. Wang, L. Sun, X. Fu, Ch. Liao and Ch. Yan , *Solid State Communications*, 115 (2000) 493.
21. G. Nabiyouni1, R. Sahraei, M. Toghiany, M. Majles and K. Hedayati, Rev.*Adv.Mater.Sci.* 27 (2011) 52.
22. A.Martynes, C.Guillen and J. Herrero ,*Appl. Surf. Sci*. ,140 (1999) 182.